PHYSICAL REVIEW A **95**, 051802(R) (2017)

Single-step fabrication of scalable multimode quantum resources using four-wave mixing with a spatially structured pump

Hailong Wang,[1] Claude Fabre,[2] and Jietai Jing[1,3,*]

[1]*State Key Laboratory of Precision Spectroscopy, School of Physics and Materials Science, East China Normal University, Shanghai 200062, China*

[2]*Laboratoire Kastler Brossel, Sorbonne Universités-UPMC, École Normale Supérieure, Collège de France, CNRS, 4 place Jussieu, 75252 Paris, France*

[3]*Collaborative Innovation Center of Extreme Optics, Shanxi University, Taiyuan, Shanxi 030006, China*

(Received 26 August 2015; revised manuscript received 16 February 2016; published 31 May 2017)

Multimode quantum resources or states, in which quantum correlations are shared and distributed among multiple parties, are important not only for fundamental tests of quantum effects but also for their numerous possible applications in quantum technologies, such as quantum imaging and quantum metrology. Here we demonstrate the single-step fabrication of a multimode quantum resource from four-wave mixing (FWM) process in hot Rb vapor using a spatially structured pump, which consists of a coherent combination of two tilted pump beams. During this FWM process, one probe beam is amplified, three conjugate and two new probe beams are generated. The measured degrees of the intensity squeezing for the four-beam case and six-beam case are around -4.1 ± 0.1 dB and -4.7 ± 0.1 dB, respectively. The generated multiple quantum correlated beams are naturally separated with distinct directions, which is crucial for sending them out to quantum nodes at different locations in quantum communication. Our scheme is compact, simple, phase insensitive, and easily scalable to larger number of quantum-correlated modes.

DOI: 10.1103/PhysRevA.95.051802

Multimode quantum state (MQS) [1–8] is a state in which quantum correlations are shared and distributed among multiple parties. For example, a multimode nonclassical frequency comb has been experimentally implemented by showing a global reduction of its quantum intensity fluctuations and the photon number quantum correlations between different parts of its frequency spectrum [1]; a multimode quantum resource made of three squeezed transverse modes has also been experimentally produced from an Optical Parametric Oscillator [2]. The well-established methods for generating MQS have been reported in the different kinds of systems [9–17]. A newly developed and promising trend for achieving scalability is to use a single multimode nonlinear process to generate in a single device a highly MQS [1,2,18–24], thus avoiding the use of the linear or nonlinear beamsplitter network, i.e., of a complex interferometric device.

A high MQS of light can also be generated in nonlinear media by an appropriate shaping of the pump beam [25]. A novel method [26,27] regarding the pump beam shaping has been theoretically proposed to create MQS between several spatial modes of the light field from a parametric down-conversion (PDC) pumped by a spatially structured pump (SSP) made of multiple symmetrically tilted plane waves. Such SSP based PDC is compact and easily scalable. It allows for both single-step fabrication of a multimode quantum resource and natural separation of its modes.

Four-wave mixing (FWM) process in a hot Rb vapor [28–37] has been used to successfully generate twin quantum correlated beams and bipartite entangled beams. It has several advantages for practical implementations, e.g., no need for a cavity due to the strong nonlinearity of the system, spatial separation of the generated nonclassical beams, and so on. Due to these advantages, it is a good candidate for generating MQS of light which has potential applications in quantum communication [38–44]. For example, very recently, theoretical proposals based on FWM in hot vapor were proposed to realize continuous variable cluster state generation over a spatial comb through the FWM process [45] and versatile quantum network generation by cascading several FWM processes [46]. In 2014, our group experimentally generated three bright, strongly quantum-correlated beams by cascading two FWM processes in hot vapors [17]. In this paper, we experimentally demonstrate a single-step fabrication of a multimode quantum resource from FWM process in hot Rb vapor with SSP. The configuration of our scheme for generating the multiple quantum correlated beams is shown in Fig. 1(a). Two strong bright pumps (Pump_1 and Pump_2), which constitute the SSP, are focused and crossed in the center of a hot ^{85}Rb vapor cell at a small angle. A coherent probe beam (Seed) is seeded into the vapor cell, where it symmetrically crosses with the two pump beams. The probe beam is red-shifted from the pump beam to match the energy diagram of the ^{85}Rb used in our previous works [17,47]. The probe beam and the two pump beams are not within the same plane, making the multiple output beams naturally separated in space. Under this configuration, first, each pump beam will interact with the probe beam individually by the single-pump FWM process [28–37]. The probe beam is amplified ($\hat{a}_1$) and two conjugate beams ($\hat{a}_2$ and $\hat{a}_4$) are simultaneously generated. Due to the phase-matching condition, a dual-pump FWM process involving both of the two pump beams is possible, in which each pump beam annihilates one photon, the probe beam gets one photon, and at the same time one photon is generated in a new conjugate beam ($\hat{a}_3$). The three FWM processes contribute to the amplification of the probe beam ($\hat{a}_1$) and the generation of the three conjugate beams ($\hat{a}_2$, $\hat{a}_3$, and $\hat{a}_4$). The new probe beam $\hat{a}_5$ ($\hat{a}_6$) is generated by the

*Corresponding author: jtjing@phy.ecnu.edu.cn

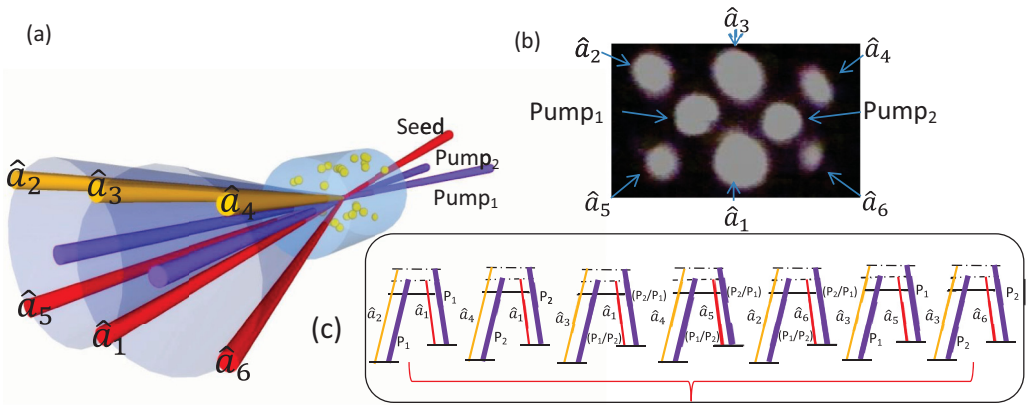

FIG. 1. Proposed scheme for generating MQS based on SSP FWM. (a) Setup of SSP FWM process. (b) The CCD camera capture of the SSP FWM output beams in the far field. Pump_1 (P_1) and Pump_2 (P_2) are filtered by Glan-Thompson polarizer at the output, $\hat{a}_1$ is the amplified probe beam, three conjugate beams ($\hat{a}_2$, $\hat{a}_3$, and $\hat{a}_4$) and two new probe beams ($\hat{a}_5$ and $\hat{a}_6$) are generated. (c) Energy level diagrams of ^{85}Rb D1 line for the SSP FWM process including seven FWM interaction.

coupling between $\hat{a}_3$ and Pump_1 (Pump_2). Another possible type of coupling is that beam $\hat{a}_4$ ($\hat{a}_2$) couples with Pump_1 and Pump_2, resulting in the generation of $\hat{a}_5$ ($\hat{a}_6$). Compared to a previous work where a Laguerre-Gauss pump was used to demonstrate the conservation of orbital angular momentum in a FWM system with only the single-pump FWM interaction involved [48], our work fully exploits both of the single-pump and dual-pump FWM interactions and thus produces six naturally separated quantum correlated beams with distinct directions. The produced multiple quantum-correlated beams are shown in Fig. 1(b). The energy diagrams for the seven FWM interactions are shown in Fig. 1(c).

The interaction Hamiltonian in the undepleted and classical pump approximation can be written as

$$\begin{aligned}\hat{H} = i\hbar[&\varepsilon_1(\hat{a}_1^\dagger\hat{a}_2^\dagger - \hat{a}_1\hat{a}_2) + \varepsilon_2(\hat{a}_1^\dagger\hat{a}_3^\dagger - \hat{a}_1\hat{a}_3) + \varepsilon_3(\hat{a}_1^\dagger\hat{a}_4^\dagger \\ &-\hat{a}_1\hat{a}_4) + \varepsilon_4(\hat{a}_3^\dagger\hat{a}_5^\dagger - \hat{a}_3\hat{a}_5) + \varepsilon_5(\hat{a}_3^\dagger\hat{a}_6^\dagger - \hat{a}_3\hat{a}_6) \\ &+\varepsilon_6(\hat{a}_4^\dagger\hat{a}_5^\dagger - \hat{a}_4\hat{a}_5) + \varepsilon_7(\hat{a}_2^\dagger\hat{a}_6^\dagger - \hat{a}_2\hat{a}_6)] \qquad (1)\end{aligned}$$

with ε_i (i=1, 2, 3, 4, 5, 6, and 7) representing the interaction strength and $\hat{a}_i$ (i=1, 2, 3, 4, 5, and 6) the bosonic annihilation operators. It can be proved that the linear combination of the photon number operators of the six beams $\hat{N}_1 - \hat{N}_2 - \hat{N}_3 - \hat{N}_4 + \hat{N}_5 + \hat{N}_6$ commutes with the Hamiltonian and is a Casimir operator, and therefore a constant of motion. The degree of squeezing (DS), i.e., the ratio of the variance of the light beams to the variance at the standard quantum limit (SQL), of the variances $\text{Var}(\hat{N}_1 - \hat{N}_2 - \hat{N}_3 - \hat{N}_4 + \hat{N}_5 + \hat{N}_6)_{\text{FWM}}$ and $\text{Var}(\hat{N}_1 - \hat{N}_2 - \hat{N}_3 - \hat{N}_4)_{\text{FWM}}$ are theoretically discussed in the Appendix in detail. The result shows that our SSP FWM scheme always squeezes the quantum noise of the linear combination of the photon number operators of the six beams below the SQL and clearly exhibits the quantum correlation shared between the six modes. However, the variance of the four-beam photon number difference operator is not always below the SQL. Therefore, modes $\hat{a}_5$ and $\hat{a}_6$ are essential to the system. In this sense, the criterion for the MQS can be characterized by the DS. When DS < 1, we could claim that MQS is generated.

Our detailed experimental setup is shown in Fig. 2 (see the experimental details in the Appendix). One of the beams from the Ti:Sapphire laser is equally divided to generate the two pump beams, i.e., the SSP, the other beam is passed through an acoustooptic modulator (AOM) to get the seed beam. The two pump beams are crossed at an angle of 11 mrad and the probe beam is symmetrically crossed with the plane of the SSP at an angle about 5 mrad in the center of the vapor cell. When both Pump_1 and Pump_2 are about 360 mW, the initial probe beam with a power of about 100 μW is amplified by a gain of $G \approx 2.3$, becoming $\hat{a}_1$, three conjugate beams ($\hat{a}_2$, $\hat{a}_3$, and $\hat{a}_4$), and two new probe beams ($\hat{a}_5$ and $\hat{a}_6$) with frequencies of 3.04 GHz blue-shifted and red-shifted from the pump are produced. The six beams, $\hat{a}_1$, $\hat{a}_2$, $\hat{a}_3$, $\hat{a}_4$, $\hat{a}_5$, and $\hat{a}_6$ have powers of about 228, 20, 131, 17, 10, and 5.5 μW under the current experimental situation. The asymmetry of the powers of modes $\hat{a}_5$ and $\hat{a}_6$ is due to the imperfection of the setup, especially the crossing angle between the probe $\hat{a}_1$ and the Pump_1 is slightly different from the angle between the probe $\hat{a}_1$ and the Pump_2. All the beams are sent to the photodetectors. The detectors' transimpedance gain is 10^4 V/A and quantum

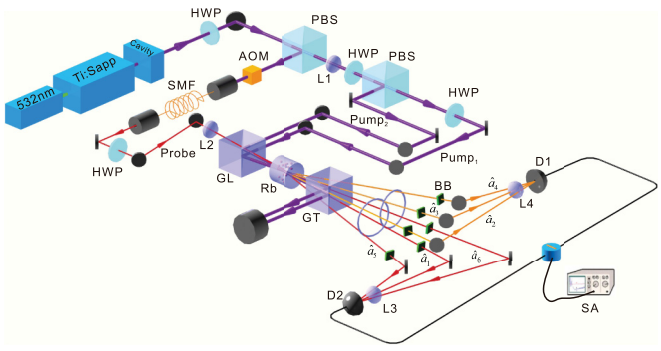

FIG. 2. Detailed experimental layout for generating and detecting the MQS. PBS, polarization beamsplitter; AOM, acoustooptic modulator; SMF, single-mode fiber; L1-L4, thin lenses; HWP, half wave plate; GL, Glan-Laser polarizer; GT, Glan-Thompson polarizer; BB, beam blocker; D1-D2, photodetectors; SA, spectrum analyzer; Pump_1-Pump_2, the SSP; $\hat{a}_1$, $\hat{a}_5$, and $\hat{a}_6$, probe beams; $\hat{a}_2$, $\hat{a}_3$, and $\hat{a}_4$, conjugate beams.

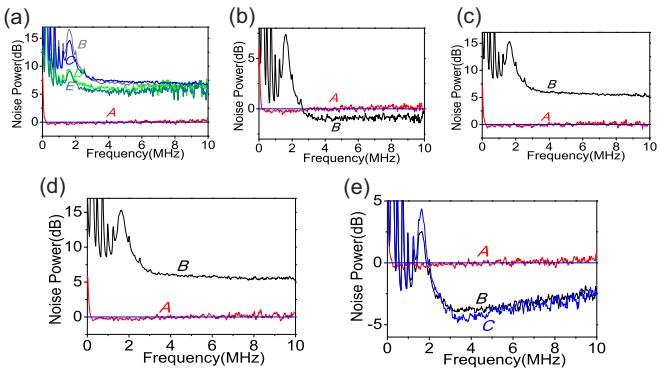

FIG. 3. Measured quantum correlations of the MQS. (a) Traces B, C, D, and E are noise power spectra of i_1, i_3, i_2, and i_4 respectively. Trace A is the normalized SQL. (b) Intensity-difference noise power spectrum of $i_1 - i_3$ (Trace B) and the corresponding SQL (Trace A). (c) Intensity-difference noise power spectrum of $i_1 - i_2$ (Trace B) and the corresponding SQL (Trace A). (d) Intensity-difference noise power spectrum of $i_1 - i_4$ (Trace B) and the corresponding SQL (Trace A). (e) Noise power spectrum of $i_1 - i_2 - i_3 - i_4$ (Trace B), $i_1 - i_2 - i_3 - i_4 + i_5 + i_6$ (Trace C) and the corresponding SQLs (Trace A); The electronic and background noise are all about 6 dB below the corresponding SQLs at 4 MHz and have been subtracted from all of the traces.

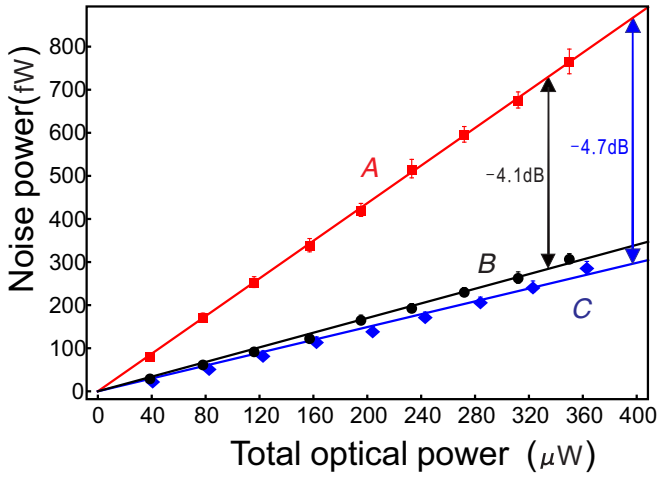

FIG. 4. Measured intensity noise power at 4 MHz for four-beam and six-beam cases. Trace A is the noise power of SQL; Trace B is the intensity noise power of four-beam case; Trace C is the intensity noise power of six-beam case, all versus total power falling on the photodetector. All these three noise power curves fit to straight lines. The electronic noise floor and background noise are subtracted from all of the data points.

efficiency is 96%. The photocurrents i_1, i_2, i_3, i_4, i_5, and i_6 indicating the photon number of beams $\hat{a}_1$, $\hat{a}_2$, $\hat{a}_3$, $\hat{a}_4$, $\hat{a}_5$, and $\hat{a}_6$ and their combinations are obtained by switching the beam blockers (BB) in front of the detectors and then analyzed with a spectrum analyser (SA). The results are shown in Fig. 3. All of these traces are normalized to the corresponding SQLs (trace A in Fig. 3), the blue straight line at 0 dB is taken as a reference, which corresponds to the average value of data points on trace A. The slight tilt of the SQL is due to the significant difference of the electronic noise level between the lower and higher frequencies.

We first record the photocurrent noise powers of i_1, i_2, i_3, and i_4 and we find that they are all above their corresponding SQLs as shown in Fig. 3(a). This is due to the amplification from the SSP FWM. The noise powers of the i_1 and i_3 are higher than the ones of i_2 and i_4, meaning they are experiencing a stronger amplification. This is consistent with the average power values mentioned above. We calibrate the SQL of the measured beams by using a beam in a coherent state with a power equal to the total power of the measured beams impinging on the photodetectors. We then split it with a 50/50 beamsplitter, direct the obtained beams into two photodetectors, D1 and D2, and record the noise power of the differential photocurrent. This balanced detection system makes it possible to cancel all the sources of classical noise and obtain a measure of the SQL. The presence of the second pump actually degrades the intensity gain of the individual single-pump FWM process due to some competition mechanism between these FWM processes. We then subtract i_3 from i_1, this is shown in Fig. 3(b), demonstrating -0.9 ± 0.2 dB intensity-difference squeezing due to their power comparability, i.e., their quantum noise comparability, which ensures good quantum noise cancellation between them and thus leads to the appearance of the quantum correlation. Figures 3(c) and 3(d) indicate that $i_1 - i_2$ and $i_1 - i_4$ show no squeezing due to their extremely unbalanced beam powers. The most interesting results are shown in Fig. 3(e), which gives the intensity noise power spectra of the four-beam case in the form of $i_1 - i_2 - i_3 - i_4$ (Trace B) and six-beam case in the form of $i_1 - i_2 - i_3 - i_4 + i_5 + i_6$ (Trace C). They are about 3.8 ± 0.2 dB and 4.2 ± 0.3 dB below their corresponding SQLs (Trace A), respectively, after accounting for the background and electronic noise. It shows that the quantum correlation of the six-beam case is enhanced from the one of the four-beam case. The large peaks shown around 1.6 MHz are classical noise from our Ti:Sapphire laser.

To better quantify the degrees of squeezing for the four-beam and six-beam cases, and show the squeezing enhancement caused by the beams $\hat{a}_5$ and $\hat{a}_6$, we measure the intensity noise powers for both four-beam and six-beam cases for our SSP FWM system (Traces B, C in Fig. 4) at 4 MHz as a function of the total optical power impinging on the photodetectors. Similarly, we also record the noise power of a coherent beam (Trace A) at different optical power using the SQL measurement method. After fitting these three noise power curves to straight lines, we find that the ratio of slopes between curves A and B is equal to 0.39 ± 0.01 which shows intensity squeezing of about -4.1 ± 0.1 dB between the four beams. After including $\hat{a}_5$ and $\hat{a}_6$, the intensity squeezing degree of six beams is enhanced to -4.7 ± 0.1 dB, which is derived from the ratio of slopes between curves A and C (0.34 ± 0.01). In this sense, the two probe beams $\hat{a}_5$ and $\hat{a}_6$ are the important components for our SSP FWM system.

Obviously, it is straightforward to shine more pump beams in the center of the vapor cell from different directions, and therefore to generate more quantum correlated beams. As shown in Fig. 5, the purple dot means the spatial location of the Pump_1 or Pump_2 at the output of the vapor cell. Similarly, the red (orange) dot means the spatial location of the probe

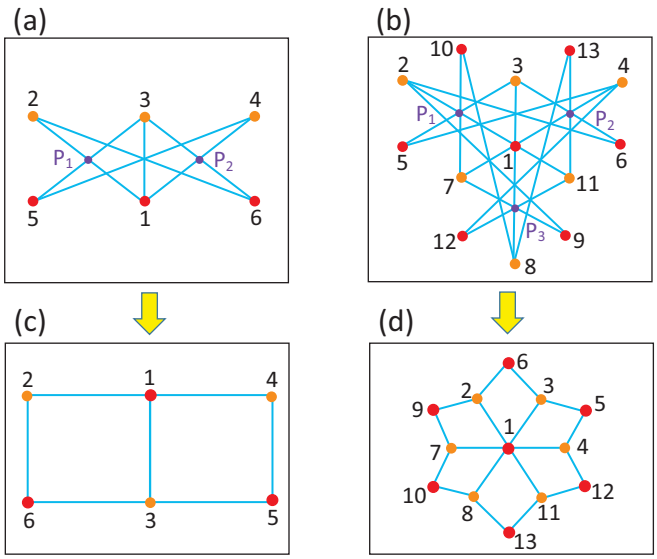

FIG. 5. Scalability of the SSP FWM for generating MQS. The purple, red, and orange dots mean the pump beam, probe beam, and conjugate beam, respectively. Numbers 1 to 13 mean the corresponding probe and conjugate beams. P_1-P_3 mean the pump beams. (a) The spatial structure of the output fields for the two-pump case. (b) The spatial structure of the output fields for the three-pump case. (c) "Ladder-type" graph showing the interaction structure of the optical fields for the two-pump case. (d) "Spider-web-type" graph showing the interaction structure of the optical fields for the three-pump case.

(conjugate) beam at the output of the vapor cell. Therefore, Figs. 5(a) and 5(b) stand for the spatial structure of the generated quantum modes at the output of the vapor cell. The blue line means the interaction between the two connected modes [49]. In this way, the connection with the purple dot means the single-pump FWM interaction while the connection without the purple dot means the aforementioned dual-pump FWM interaction, in which each pump beam annihilates one photon, the probe beam gets one photon, and at the same time, one photon is generated in a new conjugate beam ($\hat{a}_3$). The generation of modes ($\hat{a}_5$ and $\hat{a}_6$) includes both the single-pump and dual-pump FWM interactions. So we connect all the modes with the two possible FWM interactions and then get this graph in Fig. 5(a). The number of quantum-correlated beams is 6 when two pump beams are involved as shown in Fig. 5(a). If we add one more pump beam which is crossed with the two previous pumps in the center of the vapor cell and connect all the possible interactions, the number of the quantum correlated beams will be increased to 13 as shown in Fig. 5(b). Under the undepleted pump approximation, these graphs representing six modes of the two-pump case in Fig. 5(a) and 13 modes of the three-pump case in Fig. 5(b) can also be sketched as Figs. 5(c) and 5(d) by omitting of the pumps and rearrangement of the probe and conjugate beams, respectively. They appear as the "ladder-type" graph [Fig. 5(c)] and "spider-web-type" graph [Fig. 5(d)], which show the interaction structures between the modes more explicitly. Our current scheme is thus very compact, simple, phase-insensitive, and easily scalable to larger numbers of quantum correlated modes. It is substantially different from our previous work based on cascaded FWM process [17] and has absolute superiority about scalability over it.

In conclusion, we theoretically propose and experimentally demonstrate a scheme for the generation of four and six quantum-correlated beams based on the SSP FWM process in hot Rb vapor. During this SSP FWM process, one probe beam is amplified, three conjugate, and two new probe beams are generated. The measured degrees of the intensity squeezing for the four-beam case and six-beam case are around -4.1 ± 0.1 dB and -4.7 ± 0.1 dB, respectively. The generated multiple quantum-correlated beams are naturally separated with distinct directions, which is crucial for sending them out to quantum nodes at different locations in quantum communication. Our scheme is compact, simple, phase insensitive, and easily scalable to larger number of quantum-correlated modes. In this experiment we measure only the intensity noises of the different beams, and not the quadrature components quantum noise and correlations. Hence, we cannot ascertain so far that the beams are entangled. To characterize entanglement, we are planning to make homodyne measurements of quadrature components [28] and ultimately to measure the full covariance matrix [50].

This work was supported by the National Natural Science Foundation of China (Grants No. 91436211, No. 11374104, and No. 10974057); Natural Science Foundation of Shanghai (17ZR1442900); the SRFDP (20130076110011); the Program for Professor of Special Appointment (Eastern Scholar) at Shanghai Institutions of Higher Learning; the Shu Guang project supported by Shanghai Municipal Education Commission and Shanghai Education Development Foundation (11SG26); Program of Introducing Talents of Discipline to Universities supported by the 111 Project (B12024); National Basic Research Program of China (2016YFA0302103); and Program of State Key Laboratory of Advanced Optical Communication Systems and Networks (2016GZKF0JT003).

APPENDIX

1. Theoretical Model

For the Hamiltonian in the main text, we make the assumption that $\varepsilon_1 = \varepsilon_3 = \varepsilon_4 = \varepsilon_5$ and $\varepsilon_6 = \varepsilon_7$ for the consideration of symmetry and simplicity. The degree of squeezing on the variance $\mathrm{Var}(\hat{N}_1 - \hat{N}_2 - \hat{N}_3 - \hat{N}_4 + \hat{N}_5 + \hat{N}_6)_{\mathrm{FWM}}$ is given by

$$\mathrm{DS} = \frac{\mathrm{Var}(\hat{N}_1 - \hat{N}_2 - \hat{N}_3 - \hat{N}_4 + \hat{N}_5 + \hat{N}_6)_{\mathrm{FWM}}}{\mathrm{Var}(\hat{N}_1 - \hat{N}_2 - \hat{N}_3 - \hat{N}_4 + \hat{N}_5 + \hat{N}_6)_{\mathrm{SQL}}} = \frac{4\varepsilon_1^2\beta^2}{\left\{\begin{array}{l}[\varepsilon_1(\alpha_2+\beta)\cosh(\alpha_1+\beta)t + \varepsilon_1(-\alpha_2+\beta)\cosh(-\alpha_1+\beta)t]^2 \\ +8\varepsilon_1^4[\cosh^2(\alpha_1 t)\sinh^2(\beta t) + \sinh^2(\alpha_1 t)\sinh^2(\beta t)] \\ +[\varepsilon_1(\alpha_2+\beta)\sinh(\alpha_1+\beta)t - \varepsilon_1(-\alpha_2+\beta)\sinh(-\alpha_1+\beta)t]^2\end{array}\right\}}$$

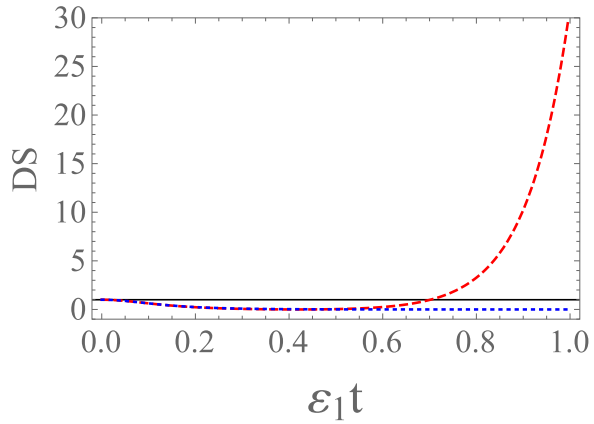

FIG. 6. The DSs of the variance $\mathrm{Var}(\hat{N}_1 - \hat{N}_2 - \hat{N}_3 - \hat{N}_4)_{\mathrm{FWM}}$ (dashed red line) and $\mathrm{Var}(\hat{N}_1 - \hat{N}_2 - \hat{N}_3 - \hat{N}_4 + \hat{N}_5 + \hat{N}_6)_{\mathrm{FWM}}$ (dotted blue line) for the case of ε_1:ε_2:ε_6=1:5:0.4. The black line: DS = 1.

where $2\alpha_1 = (\varepsilon_2 + \varepsilon_6), 2\alpha_2 = (\varepsilon_2 - \varepsilon_6), \beta = \sqrt{2\varepsilon_1^2 + \alpha_2^2}$. DS, i.e., "degree of squeezing", which is the ratio of the variance of the light beams to the variance at the standard quantum limit (SQL). In this sense, the criterion for the multimode quantum state (MQS) can be characterized by the DS. MQS will be present only when DS < 1. The DS of the variance $\mathrm{Var}(\hat{N}_1 - \hat{N}_2 - \hat{N}_3 - \hat{N}_4)_{\mathrm{FWM}}$ can be obtained by neglecting the contributions from the modes $\hat{a}_5$ and $\hat{a}_6$. The results are shown in Fig. 6.

As shown in Fig. 6, our SSP FWM scheme always squeezes the quantum noise of the photon number difference operator for six-beam case (dotted blue line) below the SQL since DS is always smaller than 1. In addition, we can see that the DS for four-beam case (dashed red line) disappears after $\varepsilon_1 t > 0.7$. The reason is as follows: the contribution of modes $\hat{a}_5$ and $\hat{a}_6$ to the quantum correlation of the six-beam case become more and more dominant with the increasing of interaction strength due to their more and more remarkable quantum amplification, thus correlation measurement of four-beam case is just a partial detection which results in the leakage of quantum correlation. From this point of view, modes $\hat{a}_5$ and $\hat{a}_6$ are essential to the system, especially when the system is operated in high gain regime.

2. Experimental Details

Figure 2 in the main text of our paper is the detailed experimental setup. The system is based on the SSP FWM process in a double $-\Lambda$ configuration in a ^{85}Rb vapor cell. We use a cavity stabilized Ti:Sapphire laser, which has a linewidth of 60 kHz tuned about 0.8 GHz to the blue of the ^{85}Rb $5S_{1/2}, F = 2 \rightarrow 5P_{1/2}$ transition with a total power of around 3600 mW. A polarizing beamsplitter (PBS) is used to split the beam. One of the beams is equally divided to generate the two pump beams, i.e., the SSP. The other beam is passed through an acousto-optic modulator (AOM). The obtained redshifted beam is then coupled into a single mode fiber (SMF) to get a good gaussian beam with TEM_{00} mode. In this way, the weak probe beam has a very good relative frequency stability with respect to the two pump beams. The Rb vapor cell is about 12 mm long and temperature stabilized at around 116°C and the windows are antireflection coated on both faces, resulting in a transmission for the probe beam of 98% per window. It is illuminated by the two intense vertically polarized pump beams with beam waists of about 550 μm ($1/e^2$ radius). The above mentioned probe beam is horizontally polarized and has a beam waist of 270 μm ($1/e^2$ radius). It is symmetrically crossed with the two pump beams in the center of the vapor cell. A Glan-Thompson polarizer (GT) with an extinction ratio of 10^5:1 at the output port of the vapor cell is used to filter out the SSP.

To verify the predicted quantum correlation between the multiple beams in our system, we measure the noise power spectra of the individual photocurrents for single beams and their particular combinations with a spectrum analyzer (SA) set to a 30 kHz resolution bandwidth (RBW) and a 300 Hz video bandwidth (VBW). This gives the variances of these photocurrents.

[1] O. Pinel, P. Jian, R. M. de Araújo, J. Feng, B. Chalopin, C. Fabre, and N. Treps, Phys. Rev. Lett. **108**, 083601 (2012).
[2] B. Chalopin, F. Scazza, C. Fabre, and N. Treps, Opt. Express **19**, 4405 (2011).
[3] M. Martinelli, N. Treps, S. Ducci, S. Gigan, A. Maître, and C. Fabre, Phys. Rev. A **67**, 023808 (2003).
[4] M. Lassen, V. Delaubert, J. Janousek, K. Wagner, H. A. Bachor, P. K. Lam, N. Treps, P. Buchhave, C. Fabre, and C. C. Harb, Phys. Rev. Lett. **98**, 083602 (2007).
[5] N. Treps, U. Andersen, B. Buchler, P. K. Lam, A. Maître, H. A. Bachor, and C. Fabre, Phys. Rev. Lett. **88**, 203601 (2002).
[6] N. Treps, N. Grosse, W. P. Bowen, C. Fabre, H. A. Bachor, and P. K. Lam, Science **301**, 940 (2003).
[7] G. J. de Valcárcel, G. Patera, N. Treps, and C. Fabre, Phys. Rev. A **74**, 061801(R) (2006).
[8] B. Chalopin, F. Scazza, C. Fabre, and N. Treps, Phys. Rev. A **81**, 061804(R) (2010).
[9] P. van Loock and S. L. Braunstein, Phys. Rev. Lett. **84**, 3482 (2000).
[10] P. van Loock and A. Furusawa, Phys. Rev. A **67**, 052315 (2003).
[11] J. Jing, J. Zhang, Y. Yan, F. Zhao, C. Xie, and K. Peng, Phys. Rev. Lett. **90**, 167903 (2003).
[12] T. Aoki, N. Takei, H. Yonezawa, K. Wakui, T. Hiraoka, A. Furusawa, and P. van Loock, Phys. Rev. Lett. **91**, 080404 (2003).
[13] H. Yonezawa, T. Aoki, and A. Furusawa, Nature (London) **431**, 430 (2004).
[14] X. Jia, Z. Yan, Z. Duan, X. Su, H. Wang, C. Xie, and K. Peng, Phys. Rev. Lett. **109**, 253604 (2012).
[15] H. Hübel, D. R. Hamel, A. Fedrizzi, S. Ramelow, K. J. Resch, and T. Jennewein, Nature (London) **466**, 601 (2010).
[16] L. K. Shalm, D. R. Hamel, Z. Yan, C. Simon, K. J. Resch, and T. Jennewein, Nat. Phys. **9**, 19 (2013).
[17] Z. Qin, L. Cao, H. Wang, A. M. Marino, W. Zhang, and J. Jing, Phys. Rev. Lett. **113**, 023602 (2014).

[18] S. Armstrong, J. F. Morizur, J. Janousek, B. Hage, N. Treps, P. K. Lam, and H. A. Bachor, Nat. Commun. **3**, 1026 (2012).
[19] C. S. Embrey, M. T. Turnbull, P. G. Petrov, and V. Boyer, Phys. Rev. X **5**, 031004 (2015).
[20] M. Pysher, Y. Miwa, R. Shahrokhshahi, R. Bloomer, and O. Pfister, Phys. Rev. Lett. **107**, 030505 (2011).
[21] S. Yokoyama, R. Ukai, S. C. Armstrong, C. Sornphiphatphong, T. Kaji, S. Suzuki, J. I. Yoshikawa, H. Yonezawa, N. C. Menicucci, and A. Furusawa, Nat. Photon. **7**, 982 (2013).
[22] J. Roslund, R. M. de Araújo, S. F. Jiang, C. Fabre, and N. Treps, Nat. Photon. **8**, 109 (2014).
[23] S. Gerke, J. Sperling, W. Vogel, Y. Cai, J. Roslund, N. Treps, and C. Fabre, Phys. Rev. Lett. **114**, 050501 (2015).
[24] M. Chen, N. C. Menicucci, and O. Pfister, Phys. Rev. Lett. **112**, 120505 (2014).
[25] G. Patera, C. N. Benlloch, G. J. de Valcárcel, and C. Fabre, Eur. Phys. J. D **66**, 241 (2012).
[26] D. Daems and N. J. Cerf, Phys. Rev. A **82**, 032303 (2010).
[27] D. Daems, F. Bernard, N. J. Cerf, and M. I. Kolobov, J. Opt. Soc. Am. B **27**, 447 (2010).
[28] V. Boyer, A. M. Marino, R. C. Pooser, and P. D. Lett, Science **321**, 544 (2008).
[29] A. M. Marino, R. C. Pooser, V. Boyer, and P. D. Lett, Nature (London) **457**, 859 (2009).
[30] Q. Glorieux, L. Guidoni, S. Guibal, J. P. Likforman, and T. Coudreau, Phys. Rev. A **84**, 053826 (2011).
[31] M. Jasperse, L. D. Turner, and R. E. Scholten, Opt. Express **19**, 3765 (2011).
[32] A. MacRae, T. Brannan, R. Achal, and A. I. Lvovsky, Phys. Rev. Lett. **109**, 033601 (2012).
[33] R. C. Pooser, A. M. Marino, V. Boyer, K. M. Jones, and P. D. Lett, Phys. Rev. Lett. **103**, 010501 (2009).
[34] R. C. Pooser and B. Lawrie, Optica **2**, 393 (2015).
[35] B. J. Lawrie, P. G. Evans, and R. C. Pooser, Phys. Rev. Lett. **110**, 156802 (2013).
[36] W. Fan, B. J. Lawrie, and R. C. Pooser, Phys. Rev. A **92**, 053812 (2015).
[37] R. C. Pooser and B. Lawrie, ACS Photonics **3**, 8 (2016).
[38] L. M. Duan, M. D. Lukin, J. I. Cirac, and P. Zoller, Nature (London) **414**, 413 (2001).
[39] S. L. Braunstein and P. van Loock, Rev. Mod. Phys. **77**, 513 (2005).
[40] D. M. Greenberger, M. A. Horne, and A. Zeilinger, *Bell's Theorem, Quantum Theory and Conceptions of the Universe*, edited by M. Kafatos, (Kluwer, Dordrecht, The Netherlands, 1989), pp. 69–72.
[41] C. Weedbrook, S. Pirandola, R. G. Patrón, N. J. Cerf, T. C. Ralph, J. H. Shapiro, and S. Lloyd, Rev. Mod. Phys. **84**, 621 (2012).
[42] M. D. Lukin, Rev. Mod. Phys. **75**, 457 (2003).
[43] J. W. Pan, Z. B. Chen, C.Y. Lu, H. Weinfurter, A. Zeilinger, and M. Żukowski, Rev. Mod. Phys. **84**, 777 (2012).
[44] H. J. Kimble, Nature (London) **453**, 1023 (2008).
[45] R. Pooser and J. Jing, Phys. Rev. A **90**, 043841 (2014).
[46] Y. Cai, J. Feng, H. Wang, G. Ferrini, X. Xu, J. Jing, and N. Treps, Phys. Rev. A **91**, 013843 (2015).
[47] F. Hudelist, J. Kong, C. Liu, J. Jing, Z. Ou, and W. Zhang, Nat. Commun. **5**, 3049 (2014).
[48] A. M. Marino, V. Boyer, R. C. Pooser, P. D. Lett, K. Lemons, and K. M. Jones, Phys. Rev. Lett. **101**, 093602 (2008).
[49] R. C. Pooser, Ph.D. thesis, University of Virginia (2007).
[50] R. Medeiros de Araujo, J. Roslund, Y. Cai, G. Ferrini, C. Fabre, and N. Treps, Phys. Rev. A **89**, 053828 (2014).